Effect of Fluorine Substitution on the Interaction of Lipophilic Ions with the Plasma Membrane of Mammalian Cells

Markus Kürschner, Katja Nielsen, Johannes R.G. von Langen, Wolfdieter A. Schenk, Ulrich Zimmermann, and Vladimir L. Sukhorukov

Lehrstuhl für Biotechnologie, Biozentrum and Institut für Anorganische Chemie der Universität Würzburg, D-97074 Würzburg, Germany

ABSTRACT The effects of the anionic tungsten carbonyl complex $[W(CO)_5SC_6H_5]^-$ and its fluorinated analog $[W(CO)_5SC_6F_5]^-$ on the electrical properties of the plasma membrane of mouse myeloma cells were studied by the single-cell electrorotation technique. At micromolar concentrations, both compounds gave rise to an additional antifield peak in the rotational spectra of cells, indicating that the plasma membrane displayed a strong dielectric dispersion. This means that both tungsten derivatives act as lipophilic ions that are able to introduce large amounts of mobile charges into the plasma membrane. The analysis of the rotational spectra allowed the evaluation not only of the passive electric properties of the plasma membrane and cytoplasm, but also of the ion transport parameters, such as the surface concentration, partition coefficient, and translocation rate constant of the lipophilic anions dissolved in the plasma membrane. Comparison of the membrane transport parameters for the two anions showed that the fluorine-substituted analog was more lipophilic, but its translocation across the plasma membrane was slower by at least one order of magnitude than that of the parent hydrogenated anion.

INTRODUCTION

Highly fluorinated organic compounds and materials, such as lipids, peptides, sugars, phenols, etc., have found a variety of biomedical applications based on the unique physicochemical properties and biological functions of fluorochemicals (Asuquo and Piddock, 1993; Devoisselle et al., 1992; O'Connell et al., 1994; Tang et al., 1997; Nöth et al., 1999). Because of their very strong intramolecular bonds and very weak intermolecular interactions, fluorocarbons (phospholipids, surfactants) exhibit exceptional chemical and biological inertness, both hydro- and lipophobicity, surface activity, aggregation, and other properties, which differ markedly from those of the parent hydrocarbons (Clary et al., 1997; Frézard et al., 1994). Clinical applications of fluorocarbons include emulsions and vesicles for delivering oxygen, genes, and monoclonal antibodies to target cells and tissues (Krafft and Riess, 1998). Fluorinated liposomal drug carriers and fluorocarbon emulsions exhibit excellent biocompatibility, low toxicity, and extended blood circulation times (Gadras et al., 1999). Compared with conventional phospholipid vesicles, fluorinated liposomes show strongly reduced membrane permeability, sharply decreased hemolytic activity, increased resistance to detergents, and a modified ability to bind negatively charged proteins and lipophilic ions (e.g., tetraphenylborate, TPB^-) (Guillod et al., 1996; McIntosh et al., 1996).

On the other hand, the substitution of fluorine for hydrogen in small molecules (including drugs, anesthetics, antibiotics, lipophilic ions, etc.) has a large influence on the interaction of these molecules with cell and model membranes (Benz, 1988; Arnold et al., 1988) and on their metabolism, cytotoxicity, and pharmacological activity (Almotrefi et al., 1993; Asuquo and Piddock, 1993; Lochhead and Zager, 1998). Valuable insight into the interactive properties of fluorochemicals has been obtained in the studies of the transport kinetics of fluorinated lipophilic ions across artificial lipid bilayers, using the charge-pulse relaxation technique (Benz, 1988). Unlike most other ions and charged molecules, lipophilic ions readily permeate lipid membranes and introduce substantial intrinsic charges within membranes, which strongly affect the electrical polarizability and conductance of lipid bilayers. The lipophilic ions adsorbed to a membrane can be used as field-sensitive molecular probes (i.e., mobile charges), which yield information about the structural and electrical properties of the membrane. The charge-pulse measurements with lipid bilayers have shown that lipophilic TPB^- derivatives with phenyl groups replaced by fluorine or trifluoromethyl ($–CF_3$) exhibit much higher translocation rates across the bilayer than the original compound (Benz, 1988). Thus the fluorine-substituted analog translocates 20 times faster and the $–CF_3$-substituted derivative almost four orders of magnitude faster than the parent TPB^-, indicating that the transmembrane mobility increases dramatically with increasing size of substituents. Although lipophilic ions have been widely used as experimental tools in studies of living cells (Turin et al., 1991; Arnold et al., 1988), little is known about the influence of structure and fluorination of lipophilic ions on their transport kinetics in biological membranes. This is because the microelectrode methods traditionally used in electrophysiological studies are restricted to

Received for publication 27 March 2000 and in final form 8 June 2000.

Address reprint requests to Prof. Dr. Ulrich Zimmermann, Lehrstuhl für Biotechnologie, Biozentrum der Universität Würzburg, Am Hubland, D-97074, Würzburg, Germany. Tel.: 49-0931-888-4507; Fax: 49-0931-888-4509; E-mail: zimmermann@biozentrum.uni-wuerzburg.de.

0006-3495/00/09/1490/08 $2.00

cells of sufficiently large size (Ryser et al., 1999) and to relatively low field frequencies because of the high impedance of microelectrodes.

The transport kinetics of lipophilic ions in the plasma membrane of small-sized cells can be studied by the single-cell electrorotation (Arnold and Zimmermann, 1982). This noninvasive AC electrokinetic technique covers a broadband frequency window (up to several hundred MHz) and therefore makes possible the investigation of a wide time range of processes. The analysis of the cell rotation spectra (i.e., frequency dependence of the cell rotation speed) with the mobile charge model (Sukhorukov and Zimmermann, 1996) allows the evaluation of the surface concentrations and translocation rate constants of the lipophilic ions adsorbed to the plasma membrane of living cells. From the rotation spectra, the passive electrical properties of the major structural units of cells, including the conductivities and permittivities of the plasma membrane, cytoplasm, cell wall, etc., can also be deduced (Zimmermann and Neil, 1996).

Recently, a number of lipophilic tungsten carbonyl anions, such as $[W(CO)_5CN]^-$ and $[W(CO)_5NCS]^-$, etc., have proved to be useful field-sensitive probe molecules for membrane structure and ion transport studies on living cells (Nielsen et al., 1996). Tungsten carbonyls were also chosen because the modular molecular design allows stepwise variation in the charge, size, shape, degree of fluorination, and chemical functions available for further derivatization. The cytotoxicity of most tungsten carbonyl anions is fairly low (Kürschner et al., 1998), which contrasts with the relatively high toxicity of large organic anions, such as the fluorinated analogs of TPB^- (Arnold et al., 1988). In this study, the interaction of the lipophilic anion $[W(CO)_5SC_6H_5]^-$ with the plasma membrane of mouse myeloma cells was compared with that of its fluorinated counterpart $[W(CO)_5SC_6F_5]^-$. The analysis of the rotation spectra of cells treated with these tungsten compounds showed that the fluorine-substituted anion bound more strongly to the membrane, but it translocated across the membrane more slowly by at least one order of magnitude than the parent hydrogenated anion.

MATERIALS AND METHODS

Synthesis of $[W(CO)_5SC_6H_5]^-$ and $[W(CO)_5SC_6F_5]^-$

The tungsten carbonyl anions (Fig. 1) used in this study were synthesized by established procedures or suitable adaptations thereof (Buchner and Schenk 1984; Kürschner et al., 1998). $Et_4N[W(CO)_5SC_6H_5]\cdot 2H_2O$ and $Et_4N[W(CO)_5SC_6F_5]$ were obtained by reacting $Et_4N[W(CO)_5Cl]$ with $NaSC_6H_5$ or $NaSC_6F_5$, respectively, in acetone/tetrahydrofuran. Compounds 1 and 2 (Fig. 1) were purified by crystallization from acetone/tetrahydrofuran and characterized by elemental analyses, IR, and ^{13}C-NMR.

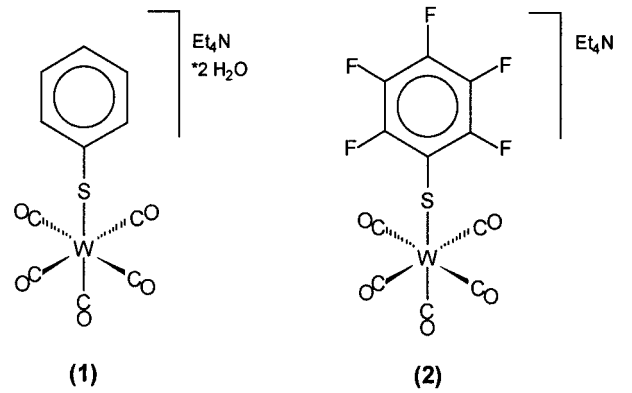

FIGURE 1 Structures of the tungsten carbonyl salts used here (formula, chemical name, formula weight of the anion): (*1*) $Et_4N[W(CO)_5SC_6H_5]\cdot 2H_2O$, tetraethylammonium pentacarbonylphenylthiolatotungstate, 433. (*2*) $Et_4N[W(CO)_5SC_6F_5]$, tetraethylammonium pentacarbonylpentafluorophenylthiolatotungstate, 523.

Cells

Mouse myeloma Sp2/0-Ag14 cells (hereafter referred to as Sp2) were cultured in complete RPMI 1640 growth medium at 37°C under 5% CO_2. Every 2–3 days, the cell suspensions were diluted by 1:10 with growth medium to keep the cells in the log phase. Before electrorotation, Sp2 cells were washed two or three times with and were resuspended in 150 mOsm inositol solutions (Sigma, Deisenhofen, Germany) at a final cell density of $1–2 \times 10^5$ cells/ml. The tungsten carbonyl compounds (Fig. 1) were added to the cell suspension at final concentrations of 0.1–50 μM, and the suspension conductivity was adjusted to 2–60 mS m^{-1} by the addition of the appropriate amounts of 150 mOsm HEPES-KOH (pH 7.4) (Sigma). To reach partition equilibrium for the adsorption of the lipophilic ions to the cell membranes, the cells were incubated with the anions for 20–40 min before electrorotation measurements. For further details see Kürschner et al. (1998).

Rotation chambers and external fields

Electrorotation spectra were measured in a microstructured four-electrode chamber, which was arranged as a planar array of circular electrodes with 60-μm diameter, 140-nm thickness (20 nm Ta and 120 nm Pt), and 200-μm electrode spacing. The microstructures were fabricated photolithographically (Fraunhofer-Institut Siliziumtechnologie, ISiT, Itzehoe, Germany). The electrodes were driven by four 90° phase-shifted, symmetrically rectangular signals from a pulse generator (HP 8130A; Hewlett-Packard, Boeblingen, Germany) with 2.5–4.8 V_{PP} amplitude over the frequency range from ~100 Hz to 150 MHz. A sample of cell suspension (50–70 μl) was added to the rotation chamber, and a coverslip was placed gently over its center. The cells were observed with a BX 50 Olympus microscope (Hamburg, Germany), and their radii were determined with a calibrated ocular micrometer. The microscope was equipped with a CCD video camera (SSC-M370CE; Sony, Cologne, Germany) connected to a video monitor. Electrorotation spectra were monitored by decreasing the field frequency in steps (5–7 frequency points/decade). At each field frequency, the rotation speed (Ω) of lone cells located near the center of the chamber was determined with a stopwatch. The rotation spectra were normalized to a field strength of 1 $V_{PP}/100$ μm and fitted with Mathematica software.

RESULTS

Rotation spectra of control cells

Electrorotation spectra of control Sp2 cells at different external conductivities (σ_e) ranging from 2 to 60 mS m^{-1} are shown in Fig. 2 (*empty circles*). The characteristic frequencies of the rotation peaks were estimated by fitting Eq. 2 (see Appendix) to the spectra (superposition of two Lorentzian curves; fits not shown). With increasing σ_e, the antifield rotation peak moved toward higher frequency from f_{c1} = 10.4 kHz at 2 mS m^{-1} to 23.6 kHz at 5 mS m^{-1} and then to 225 kHz at 60 mS m^{-1}. This low-frequency peak is due to the capacitive charging of the plasma membrane (Arnold and Zimmermann, 1982; Jones, 1995; Gimsa and Wachner, 1998). Field frequencies above 1 MHz gave cofield rotation caused by the polarization of the conductive cytosol. The characteristic frequency f_{c2} of the cytosolic peak was less sensitive to σ_e. The f_{c2} values of control cells were 16.2, 25.3, and 55.8 MHz at 2, 5, and 60 mS m^{-1}, respectively. At high conductivity (60 mS m^{-1}; Fig. 2 *C*), a distinctive asymmetry occurred in the antifield part of the rotation spectrum. As shown elsewhere (Kürschner et al., 1998), this alteration of the antifield peak resulted from the cytosolic dispersion of Sp2 cells, which was mainly due to the structural "Maxwell-Wagner" polarization of their large nucleus. Under low-conductivity conditions (σ_e = 2–5 mS m^{-1}), the nucleus did not significantly affect the rotation spectra of control cells (Fig. 2, *A* and *B*). The continuous curves in Fig. 2 represent the theoretical spectra calculated with model 2 (a single-shelled cell with a dispersion of the cytosol) that best fit to the data of control cells. Curve fitting of individual spectra yields the following ranges for the plasma membrane capacitance C_m and conductance G_m, as well as for the cytosolic permittivities ϵ_i and conductivities σ_i at high (subscript h) and low (subscript l) frequencies: C_m = 6.5–6.9 mF m^{-2}, G_m = 10–100 S m^{-2}, σ_{il} = 0.25–0.38 S m^{-1}, σ_{ih} = 0.32–0.58 S m^{-1}, ϵ_{ih} = (120–130)ϵ_0; the cytosolic dispersion was centered at f_d = 2–4 MHz. The values of the internal conductivities (σ_{il} and σ_{ih}) decreased gradually with decreasing external conductivity. This was clearly due to ion leakage from the cytoplasm of cells, which were exposed to hypotonic low-salinity electrorotation media for 20–40 min.

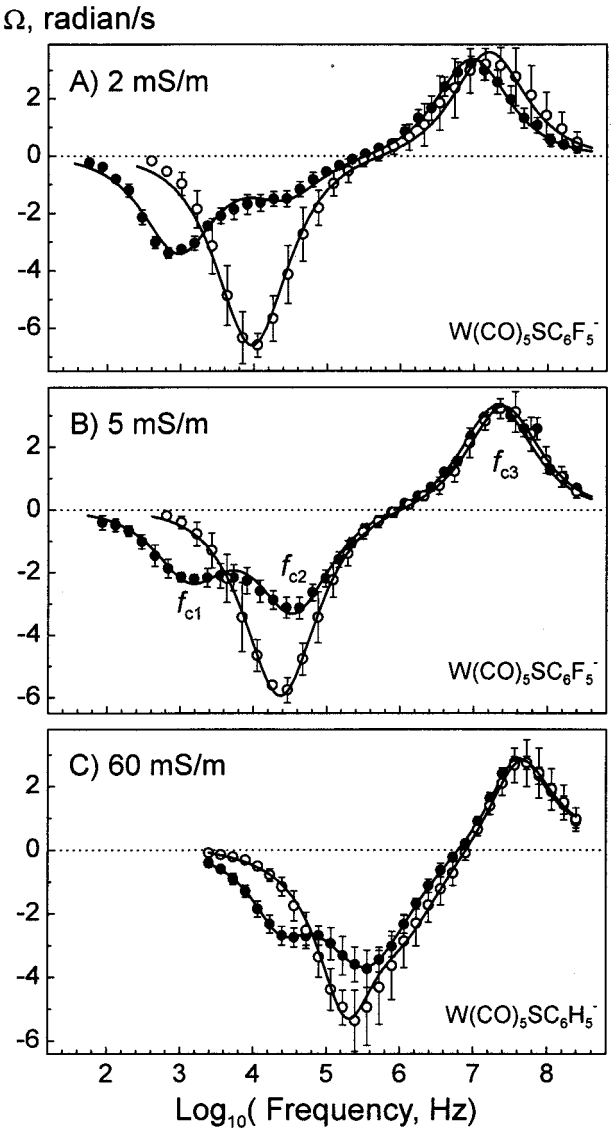

FIGURE 2 Experimental rotational spectra of control Sp2 cells (○) and those treated with 5 μM $[W(CO)_5SC_6F_5]^-$ (*A* and *B*, ●) or with 50 μM $[W(CO)_5SC_6H_5]^-$ (*C*, ●) measured at different external conductivities: 2, 5, and 60 mS m^{-1} (*A*, *B*, and *C*, respectively). Each spectrum is the mean (± SD) obtained from three to six cells. The mean radius of cells was 9.6 ± 1.1 μm. The curves are best least-square fits of model 2 (control) and model 3 (treated cells) to the data. The characteristic frequencies f_{c1}, f_{c2}, and f_{c3} (*B*, ●) represent the mobile charges, plasma membrane, and cytosolic peaks, respectively. For the mobile charges and cell parameters derived by curve fitting, see text.

Effect of tungsten carbonyl anions on electrorotation spectra

The treatment of Sp2 cells with the anion $[W(CO)_5SC_6H_5]^-$ and its fluorinated analog $[W(CO)_5SC_6F_5]^-$ resulted in considerable conductivity-dependent changes of the antifield rotation, i.e., in the part of the spectrum that is influenced by the electrical properties of the plasma membrane (Fig. 2, *filled circles*). In contrast to control cells, the rotational spectra of which exhibited a single antifield peak, the spectra of cells treated with 5 μM $[W(CO)_5SC_6F_5]^-$ displayed an additional antifield maximum centered at ~1 kHz (Fig. 2, *A* and *B*). This low-frequency peak is dominated by the relaxation of mobile charges within the plasma membrane (Sukhorukov and Zimmermann, 1996). The spectra of cells observed in the presence of both anions could be approximated very accurately by a superposition of three Lorent-

zian curves (correlation coefficients $r > 0.994$, fits not shown in Fig. 2). From the fitting curves the magnitudes (R_1, R_2, and R_3) and characteristic frequencies (f_{c1}, f_{c2}, and f_{c3}) of the three maxima (mobile charges, plasma membrane, and cytosol peaks, respectively) could be evaluated. At the lowest conductivity ($\sigma_e = 2$ mS m^{-1}, Fig. 2 *A*), the mobile charge peak centered at $f_{c1} = 930$ Hz, with a magnitude of $R_1 = -3.3$ radian s^{-1}, dominated the antifield rotation, whereas the plasma membrane peak appeared at $f_{c2} = 27.5$ kHz, and its induced rotation was much slower, $R_2 = -1.3$ radian s^{-1}. At higher conductivity (5 mS m^{-1}, Fig. 2 *B*), the shape of the rotation spectrum of cells treated with $[W(CO)_5SC_6F_5]^-$ differed markedly from that observed at 2 mS m^{-1} (Fig. 2 *A*). The antifield part of the rotation spectrum measured at 5 mS m^{-1} was dominated by the plasma membrane peak at $f_{c2} = 34.8$ kHz ($R_2 = -3.2$ radian s^{-1}), whereas the magnitude of the mobile charge peak centered at $f_{c1} = 1.35$ kHz was reduced to $R_1 = -2.1$ radian s^{-1}. With increasing medium conductivity, the magnitude of the mobile charge peak was further decreased (data not shown). The cytosolic cofield maximum was not significantly affected by the treatment with $[W(CO)_5SC_6F_5]^-$.

The mobile charge model (model 3 in the Appendix) provided a good approximation to the rotation spectra of cells obtained in the presence of $[W(CO)_5SC_6F_5]^-$. The following mobile charge and cellular parameters were derived by fitting model 3 to the data shown in Fig. 2, *A* and *B* (*fitting curves* to *filled circles*): $N_t = 25$ nmol m^{-2}, $k_i = (7–9) \times 10^3$ s^{-1}, $C_m = 8$ mF m^{-2}, $G_m = 100$ S m^{-2}, $\sigma_i = 0.14–0.3$ S m^{-1}, $\epsilon_i = (110–115)\cdot\epsilon_0$. At these low conductivities, the cytosolic dispersion could be neglected.

For Sp2 cells treated with 50 μM nonfluorinated anion $[W(CO)_5SC_6H_5]^-$, the dependence of the three rotation peaks on suspension conductivity was qualitatively similar to the results obtained from cells treated with its fluorine-substituted analog. In the case of the hydrogenated anion, however, two well-resolved antifield peaks could be observed at much higher anion concentrations and at much higher external conductivities, e.g., at $c = 50$ μM and $\sigma_e = 60$ mS m^{-1} (Fig. 2 *C*). At lower conductivity (<40 mS m^{-1}) the mobile charge peak dominated the rotation spectra, whereas the plasma membrane peak was negligible (data not shown). The spectra of cells treated with $[W(CO)_5SC_6H_5]^-$ could also be fitted very accurately with model 3 (see Appendix). From the fits of individual spectra averaged in Fig. 2 *C*, the following parameters were derived: $N_t = 9.9–11.6$ nmol m^{-2}, $k_i = (0.7–1.3) \times 10^5$ s^{-1}, $C_m = 7.0–8.5$ mF m^{-2}, $G_m = 100$ S m^{-2}, $\sigma_{il} = 0.2–0.25$ S m^{-1}, $\sigma_{ih} = 0.3–0.45$ S m^{-1}, $f_d = 1–2.5$ MHz, $\epsilon_{ih} = (80–110)\cdot\epsilon_0$. Note that the translocation rate constant k_i of $[W(CO)_5SC_6H_5]^-$ was much higher than that of its fluorinated analog.

Effect of different concentrations of lipophilic anions on electrorotation spectra

Fig. 3 shows the rotation spectra of Sp2 cells treated with different concentrations of the fluorinated compound $[W(CO)_5SC_6F_5]^-$. Both spectra were obtained on individual cells at an external conductivity of ~5 mS m^{-1}. The rotation spectrum of untreated cells at this conductivity is depicted in Fig. 2 *B* (*empty circles*). In the presence of 1 μM $[W(CO)_5SC_6F_5)]^-$ (Fig. 3, *empty circles*), the plasma membrane peak ($f_{c2} = 41$ kHz, $R_2 = -3.4$) dominated the antifield rotation, whereas the magnitude of the mobile charge maximum was relatively small ($R_1 = -2.1, f_{c1} = 2.2$ kHz). The increase in the anion concentration from 1 to 10 μM resulted in the appearance of two well-resolved antifield peaks of approximately equal magnitudes (Fig. 3, *filled circles*): $f_{c1} = 1.2$ kHz ($R_1 = -2.2$, caused by the adsorbed anion) and $f_{c2} = 38.8$ kHz ($R_2 = -2.7$, due to the passive electrical properties of the plasma membrane). The anion $[W(CO)_5SC_6H_5]^-$ showed qualitatively similar concentration effects on the rotation spectra of Sp2 cells.

DISCUSSION

Dielectric dispersion of the plasma membrane caused by the lipophilic anions

In this study, single-cell electrorotation experiments were performed on mammalian cells treated with two structural analogs of tungsten pentacarbonyl $[W(CO)_5SC_6F_5]^-$ and $[W(CO)_5SC_6H_5]^-$. The analysis of the rotational spectra using the previously proposed mobile charge model (Sukhorukov and Zimmermann, 1996) allowed the evaluation not only of the passive electric properties in terms of con-

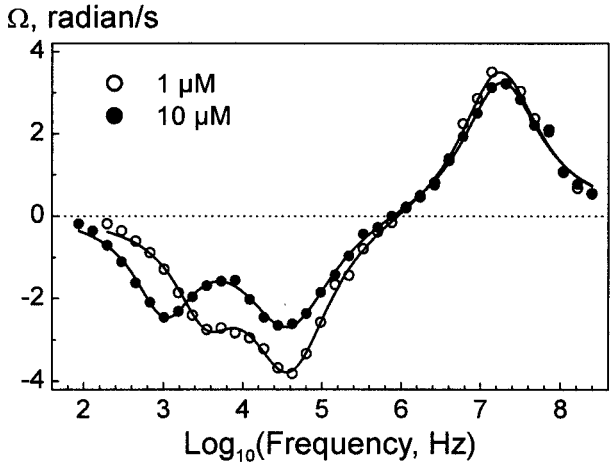

FIGURE 3 Rotation spectra of individual Sp2 cells in the presence of 1 and 10 μM of $[W(CO)_5SC_6F_5]^-$ (○ and ●, respectively). The spectra were measured at a conductivity of 5 mS m^{-1}. The mobile charge parameters are $N_t = 8.3$ nmol m^{-2} and $k_i = 1.6 \times 10^4$ s^{-1} for the 1 μM data and $N_t = 38.8$ nmol m^{-2} and $k_i = 0.6 \times 10^4$ s^{-1} for the 10 μM data.

ductivity and permittivity of the plasma membrane and cytoplasm, but also of the surface concentrations and translocation rate constants of the lipophilic anions adsorbed to the cell membrane. The partition of the lipophilic anions did not significantly alter the passive electrical properties of Sp2 cells, i.e., the values of C_{mh}, G_{ml}, ϵ_{ih}, and σ_{il} measured on cells in the presence of the anions were very similar to those obtained from the rotation spectra of control cells (Fig. 2). This is in agreement with the earlier observation that the lipophilic tungsten carbonyl compounds do not markedly affect the integrity of cell membranes and the viability of mammalian cells (Nielsen et al., 1996; Kürschner et al., 1998).

The results presented in Fig. 4 reveal considerable differences in both partition coefficients and translocation rates between the two tungsten anions studied here. From these data, the increments ΔC_m and characteristic frequencies f_{mc} of the membrane dispersion caused by the anions could be calculated. Note that the translocation rates k_i (and f_{mc}) of both ions were independent of the external conductivities, at least within the conductivity range used in this study. At a concentration of 10 μM, the anion $[W(CO)_5SC_6H_5]^-$ gave rise to a membrane dispersion centered at $f_{mc} = 32$ kHz with $\Delta C_m = 15$ mF m^{-2}, whereas the fluorinated analog relaxed at a much lower frequency of $f_{mc} = 1.3$ kHz, but the magnitude of this dispersion, $\Delta C_m = 65$ mF m^{-2}, was much higher. This also means that the fluorinated anion $[W(CO)_5SC_6F_5]^-$ gave a 10-fold increase in the apparent membrane capacitance (or its permittivity ϵ_m) at low field frequencies, from ~7 mF m^{-2} in control cells to 72 mF m^{-2} in $[W(CO)_5SC_6F_5]^-$-treated cells.

Effect of fluorination on the transport of $W(CO)_5$ derivatives through the plasma membrane

To compare the lipophilicity and transmembrane mobility of $[W(CO)_5SC_6F_5]^-$ to those of $[W(CO)_5SC_6H_5]^-$, electrorotation measurements were performed in which the external concentrations of the anions c were varied over a wide range from 0.1 to 50 μM. From the electrorotation spectra of the individual cells (similar to those shown in Figs. 2 and 3), the specific surface concentration N_t, the partition coefficient $\beta = N_t/2c$, and the translocation rate constant k_i of the lipophilic anions within the plasma membrane could be derived (Fig. 4). For both tungsten compounds, the N_t value increased and the partition coefficient β decreased gradually with increasing concentration c of the anions in the aqueous phase (Fig. 4, *A* and *B*). The decrease in β was probably caused by the generation of boundary potentials (Benz, 1988). At a given external concentration c of 5 μM, the partition coefficient for $[W(CO)_5SC_6F_5]^-$ ($\beta = 1.97$ μm) was a factor of 6 larger than that of $[W(CO)_5SC_6H_5]^-$ ($\beta = 0.33$ μm), indicating that fluorination rendered the ion much more lipophilic/less hydrophilic.

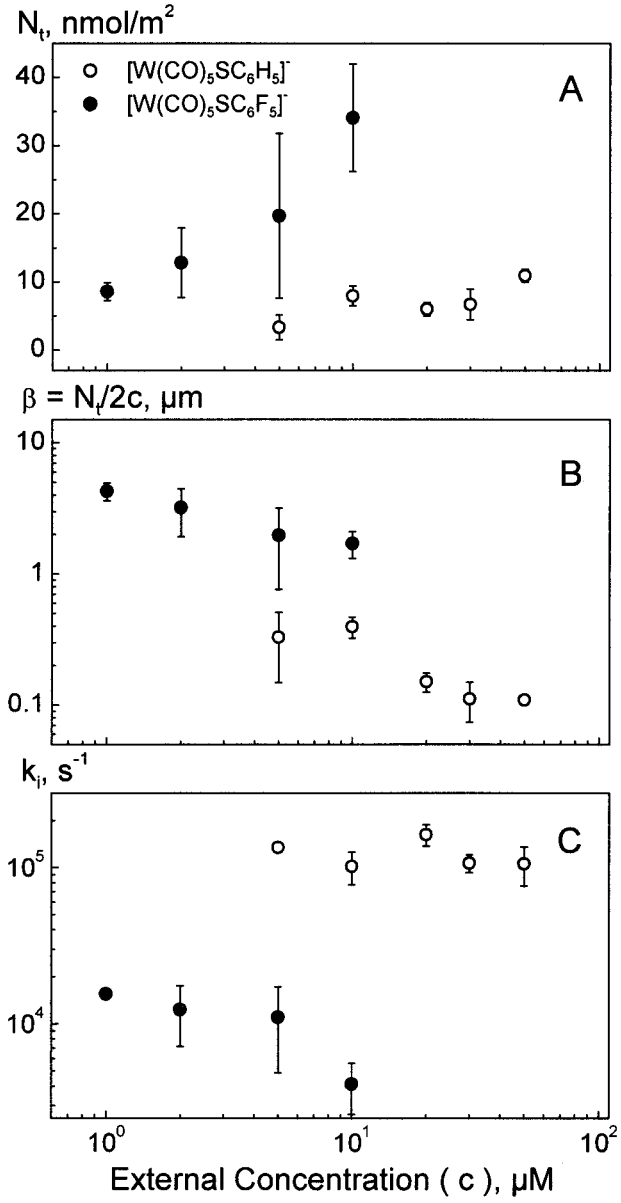

FIGURE 4 The area-specific concentration N_t and translocation rate constant k_i for the anions $[W(CO)_5SC_6H_5]^-$ and $[W(CO)_5SC_6F_5]^-$ (○ and ●, respectively) within the plasma membrane of Sp2 cells as functions of the bulk anion concentration c. The data were derived from electrorotation spectra of cells (as shown in Figs. 2 and 3).

The translocation rate constants k_i for the two anions across the cell membrane are compared in Fig. 4 *C*. The k_i value of $(0.4–1.6) \times 10^4$ s^{-1} obtained for $[W(CO)_5SC_6F_5]^-$ was at least one order of magnitude smaller than $k_i = (1–1.6) \times 10^5$ s^{-1} measured for $[W(CO)_5SC_6H_5]^-$, i.e., the fluorine-substituted anion translocated across the membrane much more slowly than its hydrogenated analog. This means that, besides the influence on lipophilicity, fluorination also reduced the transmembrane mobility of the lipophilic ions. With increasing anion concentration c, the

translocation rate of $[W(CO)_5SC_6H_5]^-$ remained nearly unchanged, whereas the saturation of membrane adsorption of the fluorinated anion $[W(CO)_5SC_6F_5]^-$ was accompanied by a gradual decrease in k_i. This may again be caused by the generation of boundary potentials, which tend to decrease both adsorption and transport kinetics of lipophilic ions (Benz, 1988).

Comparison with literature data

Comparison of the transport parameters for the hydrogenated anion $[W(CO)_5SC_6H_5]^-$ ($k_i = (1.0–1.6) \times 10^5\ s^{-1}$, $\beta = 0.11–0.4\ \mu m$) obtained here and those for its nearest and "lengthy" analog $[W(CO)_5SCH_2C_6H_5]^-$ ($k_i = (0.7–1.3) \times 10^5\ s^{-1}$, $\beta = 0.16–1.2\ \mu m$) reported earlier (Kürschner et al., 1998) shows that the larger anion is somewhat slower and more lipophilic. Nevertheless, the hydrocarbon spacer inserted between the aromatic ring and the thiolate group has little effect on the translocation rate and lipophilicity. In contrast, the properties of the interaction of the anion $[W(CO)_5SC_6H_5]^-$ with cell membranes are strongly affected by the oxidation of the thiolate bridge that associates its tungsten pentacarbonyl and phenol moieties. Thus the anion $[W(CO)_5SO_2C_6H_5]^-$, which contains sulfinate, is not able to introduce mobile charges into the plasma membrane that are detectable by electrorotation (Kürschner et al., 1998). The lack of mobile charges means that 1) the oxidized anion does not adsorb to the plasma membrane of mammalian cells and/or 2) it translocates too slowly for determination by the electrorotation technique.

The observation made in this study that the lipophilic anion with a higher translocation rate (i.e., $[W(CO)_5SC_6H_5]^-$) exhibited a much smaller partition coefficient than its slower analogs (i.e., $[W(CO)_5SCH_2C_6H_5]^-$ and $[W(CO)_5SC_6F_5]^-$) is in accord with the results obtained with a series of halogen-substituted TPB^- derivatives dissolved in artificial lipid bilayers (Benz, 1988). As pointed out elsewhere (Benz and Läuger, 1977), this relationship between β and k_i may result from small shifts of the adsorption planes of the analogs as a consequence of their different solubilities in the membrane interior. It is noteworthy that there is a good correlation between the toxicities of the TPB^- analogs in yeast cells and their translocation rate constants measured in artificial bilayers (Arnold et al., 1988), which suggests that the rate of the ion transport across the cell membrane dominates the cytotoxicity of TPB^- derivatives.

On the other hand, the effect of fluorination on the k_i values of the $W(CO)_5$ derivatives studied here and elsewhere (Kürschner et al., 1998) differed in principle from that observed with the fluorine-substituted TPB^- analogs (Benz, 1988). As already mentioned, the complete substitution of fluorine for hydrogen in the aromatic ring of $[W(CO)_5SC_6H_5]^-$ reduced the k_i value by about one order of magnitude (Fig. 4 *C*). In contrast to the $W(CO)_5$ derivatives, the introduction of a single fluorine into the phenyl rings of TPB^- leads to a 20-fold faster anion translocation across an artificial lipid bilayer (Benz, 1988). The dramatic increase in the translocation rates is explained by the larger molecular size of the fluorinated TPB^- analog as compared to the parent TPB^-. This is because bulkier ions require less Born energy to bring them from the high dielectric aqueous phase into the poorly polarizable lipid bilayer (Benz, 1988). The exactly opposite effect of fluorination on the translocation rate of the $W(CO)_5$ derivative (Fig. 4 *C*) was most likely due to the nonspherical shape of this lipophilic anion. Apparently, because of the asymmetrical charge distribution in the $[W(CO)_5SC_6F_5]^-$ molecule, the introduced fluorine atoms did not appear to mask the charged portion of the anion as efficiently as do the fluorines or trifluoromethyls attached to all four aromatic groups of the spherical TPB^- anion. Taken together, the results presented here (Fig. 4) and elsewhere (Benz, 1988) suggest that the molecular shape is an essential factor for the fast transmembrane movement of charged species.

Our finding that the solubility of the fluorinated anion in the plasma membrane was greater than that of the parent hydrogenated compound (Fig. 4, *A* and *B*) agrees with the observations reported in the literature that fluorination of various classes of drugs markedly increases their hydrophobicity. Thus introduction of fluorine into the phenol or amide group of paracetamol enhances the lipophilicity and analgesic activity of this drug (Barnard et al., 1993). The degree of fluorination of nitrobenzenes has been reported to correlate well with their ability to interact with the sulfhydryl groups located in the hydrophobic surrounding of the plasma membrane of leukocytes (Elferink and Deierkauf, 1984). The higher intracellular concentration of fluorinated colchicine derivatives has also been attributed to their stronger hydrophobicity (Ringel et al., 1991).

CONCLUSIONS

In this study the electrorotation technique has proved to be able to yield quantitative data not only on the passive electrical properties of the plasma membrane and cytosol, but also on the partition and transport kinetics of lipophilic anions in the plasma membrane of mammalian cells. The lipophilic tungsten carbonyl compounds evaluated here appear to provide a promising class of field-sensitive molecular probes for the analysis of changes in the membrane properties during cell differentiation and osmotic and chemical challenge. The data show that both adsorption and translocation properties of the fluorinated lipophilic anion differ significantly from those of its hydrogenated analog. The results of this study also offer valuable insights into the relationships between the molecular structure and membrane permeability and into the mechanisms of various processes, such as assisted and unassisted ion transport, charge transfer and stabilization inside biological mem-

branes, drug delivery, etc. Furthermore, the fluorinated lipid-soluble derivatives of $W(CO)_5$, such as $[W(CO)_5SC_6F_5]^-$, might also be of interest as contrast agents for NMR studies of biological cells, because the high sensitivity of the ^{19}F NMR imaging and spectroscopy makes it possible to easily identify these fluorinated anions adsorbed to cell membranes.

APPENDIX: THEORETICAL CONSIDERATIONS

Rotation theory

The electrorotation spectra of biological cells are fully determined by their effective polarizability f_{CM} (the Clausius-Mosotti factor), which is given by $f_{CM} = (\epsilon_p^* - \epsilon_e^*)/(\epsilon_p^* + 2\epsilon_e^*)$ (Jones, 1995; Müller et al., 1999; Schnelle et al., 1999). The complex permittivity of particles (subscript p) and external media (subscript e) with frequency-independent parameters ϵ (real permittivity) and σ (real conductivity) are defined as $\epsilon^* = \epsilon - j\sigma/\omega$, where ϵ and σ are given in [F m^{-1}] and [S m^{-1}], respectively; $j = (-1)^{1/2}$; and $\omega = 2\pi f$ is the radian field frequency. Rotation spectra of a biological cell consist of a set of co- and antifield rotation maxima. These complex spectra can be explained by modeling cells as single- or multiple-layered spheres, as shown below for three different cases: 1) The electrical properties of all cellular compartments (plasma membrane, cytoplasm, nucleus, etc.) can be assumed to be frequency independent (nondispersive model). 2) Additional maxima or shoulders in the rotation spectra of cells arise when the electrical properties of cellular components are frequency dependent (dispersive). 3) Dispersions of the plasma membrane may be induced by the adsorption of lipophilic ions (Sukhorukov and Zimmermann, 1996). The simplest single-shell model (model 1) matched well the rotation spectra of control Sp2 cells in low-conductivity solutions ($\sigma_e < 5$ mS m^{-1}). However, for higher medium conductivity and for cells treated with lipophilic anions, more complicated dispersive models had to be introduced (models 2 and 3).

Single-shell nondispersive model (model 1)

In the single-shell model, a cell is approximated by a homogeneous, conductive sphere of radius a surrounded by a low conducting shell of thickness d, corresponding to the membrane. Taking into account that $d \ll a$, a simplified expression for the complex permittivity, $\epsilon_p^* = C_m^* a \cdot \epsilon_i^*/(C_m^* a + \epsilon_i^*)$, of such a particle can be derived (Kürschner et al., 1998), where ϵ_i^* is the complex permittivity of the cytosol and C_m^* is the complex membrane capacitance per unit area, given by $C_m^* = C_m - jG_m/\omega$, where $C_m = \epsilon_m/d$ and $G_m = \sigma_m/d$ are the specific membrane capacitance [F m^{-2}] and conductance [S m^{-2}], respectively.

Single-shell model with dispersive cytosol (model 2)

A reasonable agreement between the rotation theory and the experimental spectra observed over a wide range of the external conductivity was achieved if control Sp2 cells were modeled as single-shelled particles with a dispersion of the cytosol. The dispersive properties of the cytosol can be described by $\epsilon_i^* = \epsilon_{ih} + (\epsilon_{il} - \epsilon_{ih})/(1 + j\omega\tau_d) + \sigma_{il}/j\omega$ (Pethig and Kell, 1987; Schwan, 1988;), where ϵ_{ih} (σ_{ih}) and ϵ_{il} (σ_{il}) are the values of the permittivity (conductivity) at high (subscript h) and low (subscript l) frequencies; $\tau_d = (2\pi f_d)^{-1}$ is the relaxation time; and f_d is the characteristic frequency of the dispersion.

Mobile charge model (model 3)

Models 1 and 2 were not applicable for fitting electrorotation spectra of Sp2 cells treated with the lipophilic anions tested here, because these models could not explain the appearance of an additional antifield rotational peak in the low-frequency range. Therefore we extended models 1 and 2 to the case of a membrane containing mobile charges (model 3) (Sukhorukov and Zimmermann, 1996). In model 3 the complex capacitance, C_m^*, of the plasma membrane is given by Eq. 1:

$$C_m^* = C_{mh} + \frac{C_{ml} - C_{mh}}{1 + j\omega\tau_{mc}} + \frac{G_{ml}}{j\omega} \quad (1)$$

where C_{mh} and C_{ml} are the high-frequency ("geometrical") and the low-frequency specific capacities of the plasma membrane, respectively; G_{ml} is the low-frequency membrane conductivity; and τ_{mc} is the time constant of the dielectric dispersion arising from the mobile charge within the membrane. The dispersion is centered at the characteristic frequency $f_{mc} = (2\pi\tau_{mc})^{-1}$. Equation 1 is based on the analysis given by Ketterer et al. (1971), who showed that adsorption of lipophilic ions to a lipid bilayer can result in a dielectric dispersion of the membrane properties. The magnitude, $\Delta C_m = C_{ml} - C_{mh}$, the characteristic frequency (f_{mc}), and the time constant (τ_{mc}) of the dispersion depend on the area specific concentration, N_t, and the translocation rate, k_i, of the adsorbed ion as follows: $\Delta C_m = N_t F^2/(2RT)$ and $k_i = \pi f_{mc} = (2\tau_{mc})^{-1}$.

Representation of rotational spectra with Lorentzian curves

The rotation spectra of cells can be represented by a superposition of two or more Lorentzian curves (Jones, 1995):

$$\Omega = \sum_{i=1}^{n} \frac{2R_i(f/f_{ci})}{1 + (f/f_{ci})^2} \quad (2)$$

where Ω is the rotation speed, n is the number of rotational peaks, and R_i and f_{ci} are the magnitudes and characteristic frequencies of the rotational peaks, respectively. For the single-shell model, the number of peaks $n = 2$, whereas the mobile charge model exhibits $n = 3$. The half-width of each rotation peak is 1.14 decade of frequency.

This work was supported by grants from the Deutsche Forschungsgemeinschaft to WAS and VLS (SCHE 209/17-1) and to UZ (Zi 99/12-1).

REFERENCES

Almotrefi, A. A., N. Dzimiri, H. Y. Aboul-Enein, and L. S. Premkumar. 1993. Synthesis and pharmacological evaluation of the antifibrillatory effect of fluorinated derivatives of carazolol and celiprolol: comparison with propranolol. *Gen. Pharmacol.* 24:721–725.

Arnold, W. M., and U. Zimmermann. 1982. Rotating-field-induced rotation and measurement of the membrane capacitance of single mesophyll cells of *Avena sativa. Z. Naturforsch.* 37c:908–915.

Arnold, W. M., U. Zimmermann, W. Heiden, and J. Ahlers. 1988. The influence of tetraphenylborates (hydrophobic anions) on yeast cell electro-rotation. *Biochim. Biophys. Acta.* 942:96–106.

Asuquo, A. E., and L. J. Piddock. 1993. Accumulation and killing kinetics of fifteen quinolones for *Escherichia coli*, *Staphylococcus aureus* and *Pseudomonas aeruginosa. J. Antimicrob. Chemother.* 31:865–880.

Barnard, S., R. C. Storr, P. M. O'Neill, and B. K. Park. 1993. The effect of fluorine substitution on the physicochemical properties and the analgesic activity of paracetamol. *J. Pharm. Pharmacol.* 45:736–744.

Benz, R. 1988. Structural requirement for the rapid movement of charged molecules across membranes. Experiments with tetraphenylborate analogues. *Biophys. J.* 54:25–33.

Benz, R., and P. Läuger. 1977. Transport kinetics of dipicrylamine through lipid bilayer membranes. Effects of membrane structure. *Biochim. Biophys. Acta.* 468:245–258.

Buchner, W., and W. A. Schenk. 1984. ^{13}C-NMR spectra of monosubstituted tungsten carbonyl complexes. The NMR *trans* influence in octahedral tungsten(0) compounds. *Inorg. Chem.* 23:132–137.

Clary, L., G. Verderone, C. Santaella, and P. Vierling. 1997. Membrane permeability and stability of liposomes made from highly fluorinated double-chain phosphocholines derived from diaminopropanol, serine or ethanolamine. *Biochim. Biophys. Acta.* 1328:55–64.

Devoisselle, J. M., J. Vion-Dury, S. Confort-Gouny, D. Coustaut, and P. J. Cozzone. 1992. Liposomes containing fluorinated steroids: an analysis based on photon correlation and fluorine-19 nuclear magnetic resonance spectroscopy. *J. Pharm. Sci.* 81:249–254.

Elferink, J. G., and M. Deierkauf. 1984. Inhibition of polymorphonuclear leukocyte functions by fluorinated nitrobenzenes. *Chem. Biol. Interact.* 52:163–172.

Frézard, F., C. Santaella, M.-J. Montisci, P. Vierling, and J. G. Riess. 1994. Fluorinated phosphatidylcholine-based liposomes: H^+/Na^+ permeability, active doxorubicin encapsulation and stability in human serum. *Biochim. Biophys. Acta.* 1194:61–68.

Gadras, C., C. Santaella, and P. Vierling. 1999. Improved stability of highly fluorinated phospholipid-based vesicles in the presence of bile salts. *J. Controlled Release.* 57:29–34.

Gimsa, J., and D. Wachner. 1998. A unified resistor-capacitor model for impedance, dielectrophoresis, electrorotation, and induced transmembrane potential. *Biophys. J.* 75:1107–1116.

Guillod, F., J. Greiner, and J. G. Riess. 1996. Vesicles made of glycophospholipids with homogeneous (two fluorocarbon or two hydrocarbon) or heterogeneous (one fluorocarbon and one hydrocarbon) hydrophobic double chains. *Biochim. Biophys. Acta.* 1282:283–292.

Jones, T. B. 1995. Electromechanics of Particles. Cambridge University Press, New York.

Ketterer, B., B. Neumcke, and P. Läuger. 1971. Transport mechanism of hydrophobic ions through lipid bilayer membranes. *J. Membr. Biol.* 5:225–245.

Krafft, M. P., and J. G. Riess. 1998. Highly fluorinated amphiphiles and colloidal systems, and their applications in the biomedical field. A contribution. *Biochimie.* 80:489–514.

Kürschner, M., K. Nielsen, C. Andersen, V. L. Sukhorukov, W. A. Schenk, R. Benz, and U. Zimmermann. 1998. Interaction of lipophilic ions with the plasma membrane of mammalian cells studied by electrorotation. *Biophys. J.* 74:3031–3043.

Lochhead, K. M., and R. A. Zager. 1998. Fluorinated anesthetic exposure "activates" the renal cortical sphingomyelinase cascade. *Kidney Int.* 54:373–381.

McIntosh, T. J., S. A. Simon, P. Vierling, C. Santaella, and V. Ravily. 1996. Structure and interactive properties of highly fluorinated phospholipid bilayers. *Biophys. J.* 71:1853–1868.

Müller, T., G. Gradl, S. Howitz, S. Shirley, Th. Schnelle, and G. Fuhr. 1999. A 3-D microelectrode system for handling and caging single cells and particles. *Biosens. Bioelectron.* 14:247–256.

Nielsen, K., W. A. Schenk, M. Kriegmeier, V. L. Sukhorukov, and U. Zimmermann. 1996. Absorption of tungsten carbonyl anions into the lipid bilayer membrane of mouse myeloma cells. *Inorg. Chem.* 35: 5762–5763.

Nöth, U., P. Gröhn, A. Jork, U. Zimmermann, A. Haase, and J. Lutz. 1999. ^{19}F-MRI in vivo determination of the partial oxygen pressure in perfluorocarbon-loaded alginate capsules implanted into the peritoneal cavity and different tissues. *Magn. Reson. Med.* 42:1039–1047.

O'Connell, T. M., S. A. Gabel, and R. E. London. 1994. Anomeric dependence of fluorodeoxyglucose transport in human erythrocytes. *Biochemistry.* 33:10985–10992.

Pethig, R., and D. B. Kell. 1987. The passive electrical properties of biological systems: the significance in physiology, biophysics and biotechnology. *Phys. Med. Biol.* 32:933–977.

Ringel, I., D. Jaffe, S. Alerhand, O. Boye, A. Muzaffar, and A. Brossi. 1991. Fluorinated colchicinoids: antitubulin and cytotoxic properties. *J. Med. Chem.* 34:3334–3338.

Ryser, C., J. Wang, S. Mimietz, and U. Zimmermann. 1999. Determination of the individual electrical and transport properties of the plasmalemma and the tonoplast of the giant marine alga *Ventricaria ventricosa* by means of the integrated perfusion/charge-pulse technique: evidence for a multifolded tonoplast. *J. Membr. Biol.* 168:183–197.

Schnelle, T., T. Müller, and G. Fuhr. 1999. Manipulation of particles, cells and liquid droplets by high frequency electric fields. *BioMethods.* 10: 417–452.

Schwan, H. P. 1988. Dielectric spectroscopy and electro-rotation of biological cells. *Ferroelectrics.* 86:205–233.

Sukhorukov, V. L., and U. Zimmermann. 1996. Electrorotation of erythrocytes treated with dipicrylamine: mobile charges within the membrane show their "signature" in rotational spectra. *J. Membr. Biol.* 153: 161–169.

Tang, P., B. Yan, and Y. Xu. 1997. Different distribution of fluorinated anesthetics and nonanesthetics in model membrane: a ^{19}F NMR study. *Biophys. J.* 72:1676–1682.

Turin, L., P. Béhé, I. Plonsky, and A. Dunina-Barkovskaya. 1991. Hydrophobic ion transfer between membranes of adjacent hepatocytes: a possible probe of tight junction structure. *Proc. Natl. Acad. Sci. USA.* 88:9365–9369.

Zimmermann, U., and G. A. Neil. 1996. Electromanipulation of Cells. CRC Press, Boca Raton, FL.